Earth and Planetary Science Letters ••• (••••) •••–•••

Contents lists available at ScienceDirect

Earth and Planetary Science Letters

www.elsevier.com/locate/epsl

Cassini radar observation of Punga Mare and environs: Bathymetry and composition

M. Mastrogiuseppe [a,b], V. Poggiali [b], A.G. Hayes [b], J.I. Lunine [b], R. Seu [a], G. Di Achille [c], R. Lorenz [d]

[a] University of Rome "La Sapienza", Via Eudossiana 18, 00184 Rome, Italy
[b] Department of Astronomy, Cornell University, 14853 Ithaca, NY, USA
[c] INAF National Institute for Astrophysics, Astronomical Observatory of Abruzzo, Teramo, Italy
[d] Johns Hopkins University, Applied Physics Laboratory, 11100 Johns Hopkins Road, Laurel, MD, USA

ARTICLE INFO

Article history:
Received 23 December 2017
Received in revised form 20 April 2018
Accepted 20 May 2018
Available online xxxx
Editor: W.B. McKinnon

Keywords:
radar
altimetry
planets
sounder
Titan
bathymetry

ABSTRACT

In January 2015 (fly-by T108), the Cassini radar observed Punga Mare, Titan's northernmost and third-largest sea, in altimetry mode during closest approach. The ground track intercepted a section of the mare and a system of channels and flooded areas connecting Punga to Kraken Mare. We use a processing technique, successfully adopted for Ligeia Mare and Ontario Lacus, for detecting echoes from the sea floor and constraining the depth and composition of these liquid bodies. We find that, along the radar transect, Punga Mare has a maximum measured depth of 110 m. The relative reduction in backscatter of the seafloor, as a function of increasing depth, suggests a liquid loss tangent of $3 \pm 1 \times 10^{-5}$. While this value is within the formal uncertainty of the loss tangent derived for Ligeia Mare, the best-fit solution is lower and is consistent with a nearly pure binary methane-nitrogen liquid with little to no ethane or higher order components. The indication of very low amounts of ethane toward the pole suggests that atmospheric processes are controlling the surface liquid composition of Titan's seas.

1. Introduction

Titan's surface has been widely mapped by the Cassini RADAR (2004–2017), a microwave remote sensing instrument able to penetrate the dense atmosphere of the moon at 2.17 cm wavelength. The Cassini radar was a multimode instrument capable to operate in active mode as a Synthetic Aperture Radar (SAR) for surface imaging, as a radar altimeter for topography measurements, as a scatterometer for surface composition and, in passive mode, as a radiometer for brightness temperature (Elachi et al., 2004). The instrument modes were activated sequentially during each fly-by to Titan, from an altitude of 100,000 km down to a 1,000 km at the closest approach, pointing the antenna in a convenient way to accomplish the targeted measurements. A detailed description of sequence planning and instrument performance is reported in West et al. (2009). A total number of 53 fly-bys dedicated to the radar observations, allowed Cassini to cover ~50% of Titan surface at <1 km resolution in SAR mode, as well as to acquire 40 topographic profiles in altimetry mode. This dataset enabled the identification and characterization of a series of geomorphologic features, including hundred meters high dunes (Mastrogiuseppe et al., 2014b), fluvial network of channels and canyons (Poggiali et al., 2016), mountains (Radebaugh et al., 2007; Mitri et al., 2010), craters (Wood et al., 2010), possible cryovolcanic features (Lopes et al., 2013) and large deposits of liquid hydrocarbons in lakes and seas. A detailed description and mapping of the Titan's polar terrains is reported in Birch et al. (2017).

The presence of standing hydrocarbons liquid bodies on Titan was revealed by Cassini on July 22nd, 2006, during the fly-by T16, when the radar mapped a collection of 10–100 km diameter lakes present in the Northern hemisphere (Stofan, 2007). Later observations revealed the existence of three northern seas, or maria: Kraken Mare, Ligeia Mare and Punga Mare (Hayes et al., 2008).

The altimetric observation acquired in May 2013 (flyby T91) over Ligeia Mare demonstrated that the Cassini RADAR can also operate as a sounder, capable of probing Titan's seas down to ~200 m, depending mainly on liquid composition (Mastrogiuseppe et al., 2014a). This was possible because of the very low microwave absorptivity of liquid hydrocarbon (methane and ethane), which has a microwave loss tangent (defined as the ratio between the imaginary and real components of the dielectric constant) that is approximately five orders of magnitude lower than seawater. This successful experiment suggested a re-design of the final targeted

E-mail address: marco.mastrogiuseppe@uniroma1.it (M. Mastrogiuseppe).

https://doi.org/10.1016/j.epsl.2018.05.033
0012-821X/

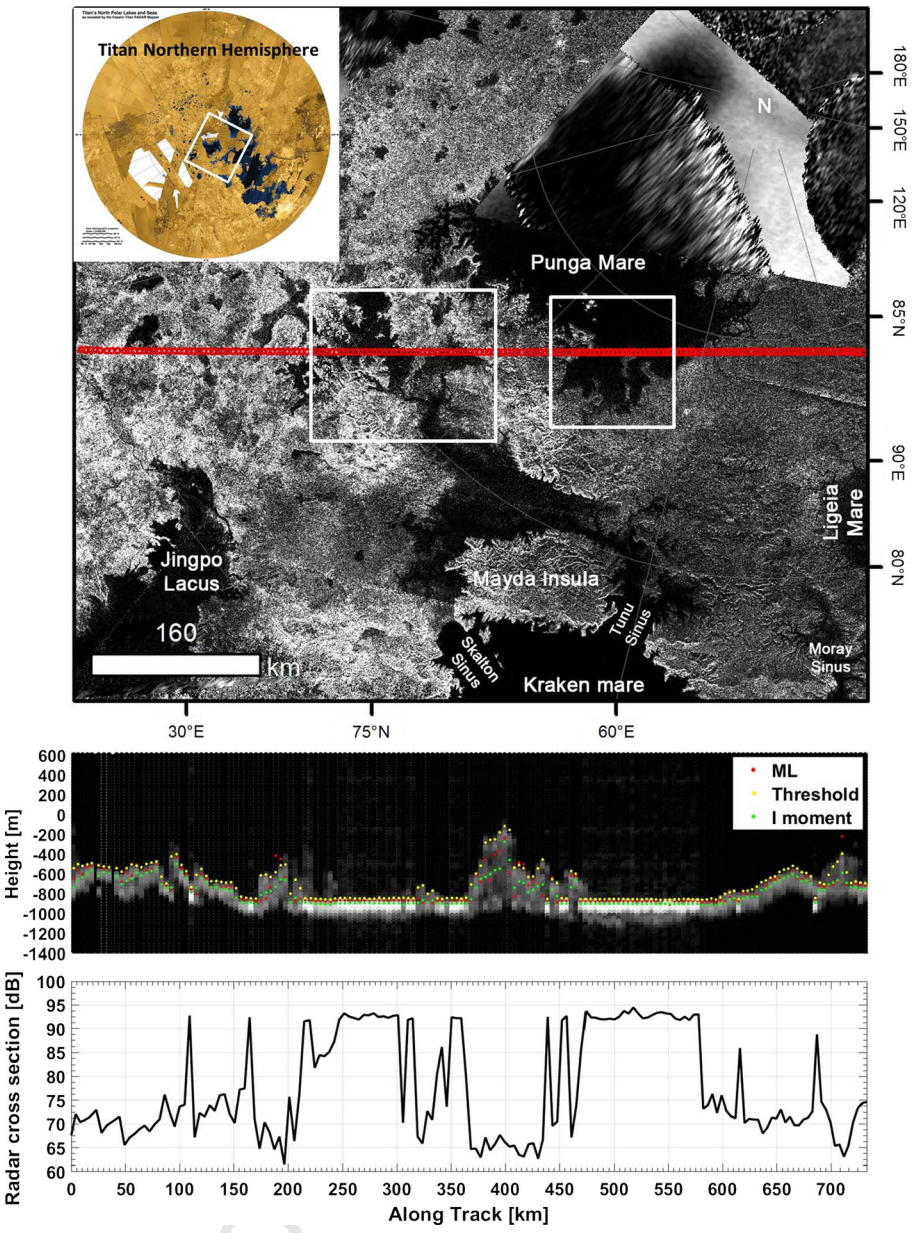

Fig. 1. (Upper panel) SAR mosaic and relative outbound altimetric 700-km-long track of flyby T108 with red circles indicating half power footprints and, in white, the two selected regions shown in Fig. 2. (Middle panel) Radargram and relative altimetry obtained using different tracking methods. (Lower panel) Radar cross section obtained from altimetry. Note that the abrupt changes to very high values of radar cross section indicate the presence of exposed liquid intercepted by the radar. (For interpretation of the colors in the figure(s), the reader is referred to the web version of this article.)

observations of Titan aimed at acquiring similar altimetry datasets over Titan's other seas in order to investigate their depth and composition. Herein, we discuss the January 11th, 2015 observation (flyby T108) of the Cassini RADAR, that acquired data over a ∼100 km long transect through Punga Mare and a portion of the flooded terrain connecting Punga and Kraken Mare during the spacecraft's closest approach to Titan, with a favorable geometry for sounding (Fig. 1 and Supplementary material).

Punga Mare has been repeatedly observed by the Cassini RADAR in its high-resolution SAR mode, notably in October 2006 (T19), April 2007 (T29) and December 2009 (T64). It is the third largest (6.1×104 km^2, Hayes, 2016) and most poleward sea on Titan (85°N, 342°W). At the time of the T108 altimetry observation, Punga Mare's surface was very smooth at the Cassini radar wavelength ($\lambda = 2.17$ cm). Investigation of the surface roughness from T108 altimetry resulted in an estimated effective σ_h (standard deviation of the surface height) ranging between 2.3 and 2.5 mm (Grima et al., 2017), consistent with a lack of wind-waves (Hayes et al., 2013). In July 2012 (T85), the Cassini Visual Infrared Mapping Spectrometer (VIMS) observed offset sun glints that were characterized as isolated patches of increased roughness consistent with wind-waves (Barnes et al., 2014). In order to produce the observed glint magnitudes, the wind-waves would have required "Significant Wave Heights" (SWH $= 4\sigma_h$) of 2^{+2}_{-1} cm (Barnes et al., 2014), consistent with wave fields generated by light winds of 0.4–0.7 m/s near the threshold for wave generation (Hayes et al., 2013).

In this paper, we adopt the dedicated radar processing technique described in Mastrogiuseppe et al. (2016) to quantitatively investigate the seafloor topography and composition of the liquid basins observed during fly-by T108. This technique has been successfully used to characterize the depth and composition of Ligeia Mare (Mastrogiuseppe et al., 2014a, 2016) and Ontario Lacus (Mastrogiuseppe et al., 2018) as reported in Table 1. A similar anal-

Please cite this article in press as: Mastrogiuseppe, M., et al. Cassini radar observation of Punga Mare and environs: Bathymetry and composition. Earth Planet. Sci. Lett. (2018), https://doi.org/10.1016/j.epsl.2018.05.033

Table 1
Depth and composition values from Cassini radar assuming a ternary methane–ethane–nitrogen composition.

Mare	Best fit / Limits (1σ)		
	Methane [%] Mean value / (1-sigma)	Nitrogen [%] Mean value / (1-sigma)	Ethane [%] Mean value / (1-sigma)
Ligeia	71 / (63-78)	17 / (14-20)	12 / (2-22)
Punga and Baffin Sinus	80 / (74-80)	20 / (18-20)	0 / (0-8)
Ontario Lacus	51 / (21-74)	11 / (05-18)	38 / (08-74)

ysis, which adopts a waveform approach, has also been used to derive Titan's solid body topography (Mastrogiuseppe et al., 2014b).

2. T108 data analysis and seafloor detection

In altimetry mode, the Cassini RADAR collected data by pointing the antenna boresight toward the center of mass of the moon, transmitting/receiving bursts of chirped signals with a pulse repetition frequency (PRF) of 5 kHz and a bandwidth of 4.25 MHz allowing a range resolution equal to 35 m in vacuum. When the radar altimeter is used as a sounder (bathymetric investigation), the range resolution is degraded to 50–60 m due to the application of custom taper functions for suppressing side lobes associated to the strong sea-surface reflection (see Supplementary material). In this work we adopt super-resolution techniques (Cuomo, 1992) to extend the standard Cassini radar bandwidth by a factor of three, allowing roughly 20 m resolution for shallow depth investigations of Titan seas and lakes.

The dedicated outbound radar altimetry observation conducted during the T108 fly-by, enabled collection of data along a 700 km ground track with spacecraft altitudes ranging from 1000 km to 1200 km above Titan's north polar terrain (Fig. 1 and Supplementary material).

During this fly-by, the antenna was pointed close to the nadir direction ($\theta < 0.035$ deg, see Supplementary Fig. S1) and its footprint intercepted the southern eastern part of Punga Mare, as well as a flooded area that connects Punga with Kraken Mare. Over the predominantly land surface of the swath, nadir glints from small patches of liquids such as small lakes and rivers, similar to those detected during the fly-by T91 (Poggiali et al., 2016), were also observed. The processing results are reported in Fig. 1, where the middle panel shows the radargram and relative altimetry of the observation and the upper panel the SAR mosaic of the region of interest. The altimetric profile obtained using conventional processing (Alberti et al., 2009), shows the presence of a complex topography where flat regions representing liquid bodies are followed by hilly regions rising hundreds of meters above the liquid surface along a slope of a few degrees. Two major liquid bodies are observed during the flyby. First, located from ~200 to 350 km along track (Fig. 1), is an estuary connected to northern Kraken Mare, hereafter simply referred to as Baffin Sinus. The second, from 470 to 570 km, is the southern part of Punga Mare. The smooth surface of both liquid bodies resulted in a very strong specular return (Fig. 1, bottom panel), permitting very precise measurements (~30–50 cm) of the distance between the spacecraft and liquid surfaces. Across the ~350 km of track over Punga Mare and Baffin Sinus, the liquid surfaces are observed to smoothly change by ~11 m (Hayes et al., 2017), consistent with estimate of Titan's geoid variability over the same track by less et al. (2012). Along with elevation measurements of Ligeia Mare and Kraken Mare, Hayes et al. (2017) used this observation to argue that Titan's Maria are connected and share a common equipotential surface (like Earth's oceans).

The results of the standard altimetric processing of the T108 radar product is shown in Supplementary Fig. S2. Radargrams show signals reflected by the smooth surface of the liquid in addition to side lobes resulting from the processing (Supplementary Fig. S2, upper panels). Reprocessing data using a custom taper function (Blackman window, Blackman and Tukey, 1959) resulted in a mitigation of side lobes (Supplementary Fig. S2, middle panels). Subsequently, we apply super-resolution technique to enhance range resolution and improve the detection of shallow (<35 m deep) subsurface echoes (see Fig. 2, bottom panel). The same technique was implemented on the T91 radar data acquired over Ligeia Mare for discriminating subsurface echoes at the shoreline of the sea (Mastrogiuseppe et al., 2014a). The result of the processing is shown in Fig. 2 (central panel) and the radargrams show the presence of echoes reflected from the seafloor of Punga Mare and nearby liquid bodies.

In Fig. 2, the lower-right panel shows a detection of liquid over the relatively small Dingle Sinus, a flooded area which connects Punga and Kraken maria. The resulting waveform shows a specular reflection from the surface followed by a weaker reflection from the subsurface. Although we applied super-resolution algorithms, the subsurface return cannot be separated from the echoes at the surface, suggesting that the depth is shallower than the limit of detection (15–20 m) after super-resolution processing.

3. Bathymetry and composition of Punga Mare and Baffin Sinus

We investigate the depth and composition of Punga Mare using the Monte Carlo approach described in Mastrogiuseppe et al. (2016). This technique, already applied to the data acquired during T91 (Mastrogiuseppe et al., 2016) and T49 flybys (Mastrogiuseppe et al., 2018), estimates the most probable values and relative uncertainties for the three parameters used for deriving the loss tangent of the liquid and bathymetry: surface to subsurface relative peak power (P_s/P_{ss}), two-way travel time of the echo ($\Delta\tau$) and subsurface roughness (σ_h).

Subsequently, the estimated values (P_s/P_{ss} and $\Delta\tau$) are used along with a parametric model for determining the specific signal attenuation K of the liquid, written as logarithmic loss per travel time as described in Mastrogiuseppe et al. (2016).

A linear regression is applied to a subset of data, including only selected bursts where the −3 dB footprint intercepted exclusively the liquid, thus not selecting the bursts where the footprints overlap the coastlines. The selection resulted in 21 footprints and in a mean value of specific attenuation $K = 13^{+5}_{-6}$ dB/μs (1-sigma uncertainty) for Punga Mare, and 17 footprints with a mean value of $K = 10^{+6}_{-8}$ dB/μs for Baffin Sinus (Supplementary Fig. S3 and Table S1).

The estimated attenuation when converted into loss tangent gives a value of $\tan\delta = 3^{+1}_{-1} \times 10^{-5}$ (1-sigma uncertainty) for Punga and $3^{+1}_{-2} \times 10^{-5}$ for Baffin Sinus.

Assuming that the liquid is composed of a ternary mixture of methane, ethane, and nitrogen, we determined the composition of the Punga Mare and Baffin Sinus using the component dielectric properties measured by Mitchell et al. (2015) and the same assumptions adopted as for Ligeia Mare and Ontario Lacus (Mastrogiuseppe et al., 2016, 2018):

1) Ethane and methane are the most abundant materials on Titan that have loss tangents low enough to match our inferred value. They are liquid under Titan conditions. (No solid compounds have the requisite low loss tangent.)

Please cite this article in press as: Mastrogiuseppe, M., et al. Cassini radar observation of Punga Mare and environs: Bathymetry and composition. Earth Planet. Sci. Lett. (2018), https://doi.org/10.1016/j.epsl.2018.05.033

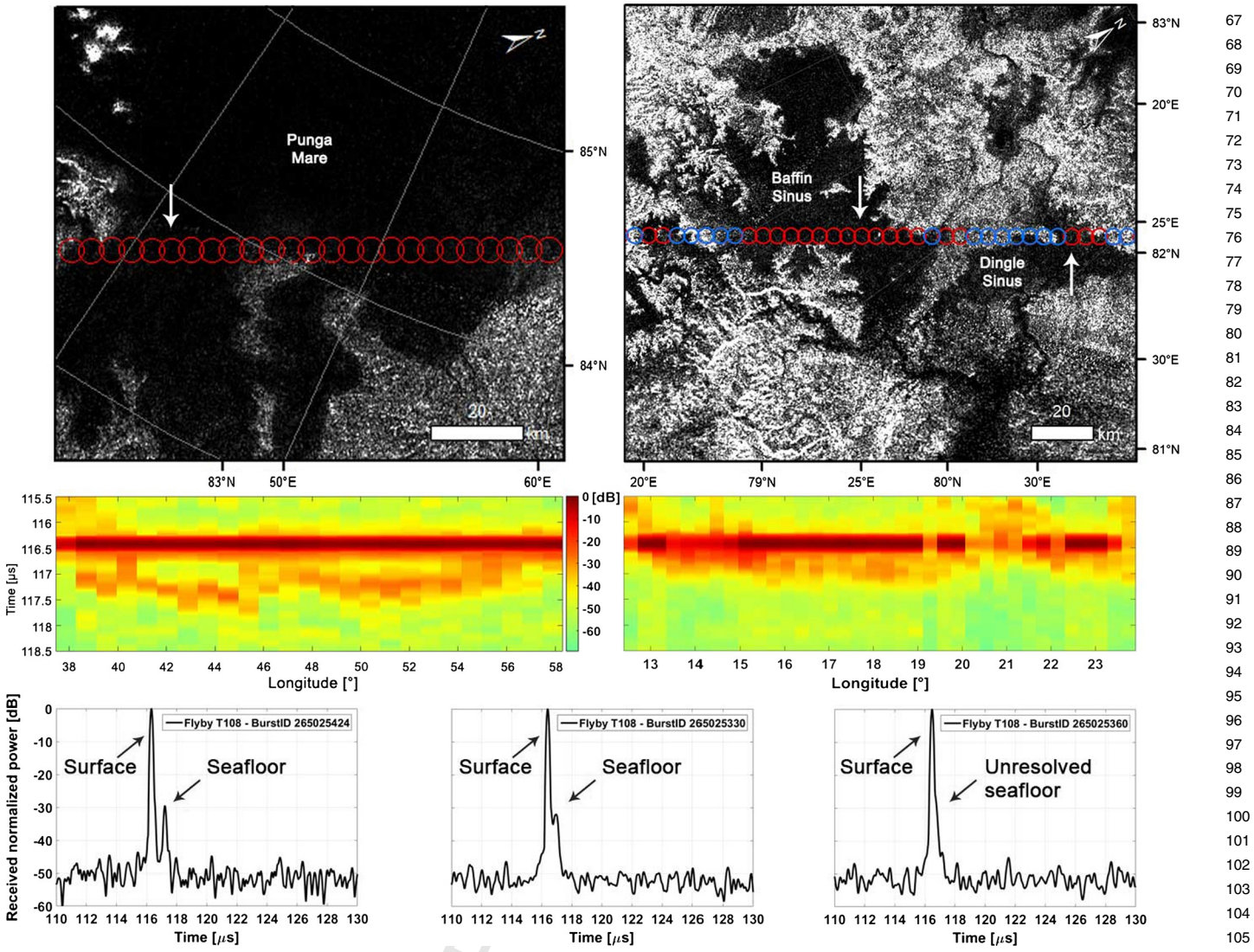

Fig. 2. (Upper panels) SAR mosaic showing the location of the −3 dB beam-limited altimeter footprints over liquid (red circles) and solid surfaces (blue circles). Note that the footprints barely overlap. (Middle panels) Super-resolved radargram: Punga mare (left) and nearby liquid bodies (right). (Bottom panels) Three waveforms received over Punga Mare (left), Baffin Sinus (middle) and Dingle Sinus (right): locations of relative footprints are indicated by white arrows.

2) Nitrogen is a dissolved component whose mole fraction in the liquid is determined by the partial pressure (1.5 bars) of nitrogen in contact with the open seas, the solubility of nitrogen measured in pure ethane and methane (Cheung and Wang, **?**), and in the binary ethane–methane system (Malaska et al., 2017).

3) The 2.18 cm wavelength microwave absorption coefficient of the mixture is a combination of its individual components as determined by Mitchell et al. (2015) using the Lorentz–Lorenz mixing rule, for nitrogen mixing ratios in methane–ethane determined by Malaska et al. (2017) assuming a temperature of 91 K. For a temperature of 95 K the ethane mole fraction will increase slightly and the nitrogen decrease.

We note that the best-fit loss tangent for Punga Mare and Baffin Sinus is close to the 3.3×10^{-5}, value given in Mitchell et al. (2015) for a purely binary mixture of methane and molecular nitrogen, with the latter's mixing ratio determined by its solubility in liquid methane under the 1.4 bar atmospheric pressure (see Malaska et al., 2017). Our best-fit composition for the observed loss tangent is therefore a binary mixture of 80% CH_4 and 20% N_2, with only trace amounts of ethane and/or high-order components which would cause higher absorption. We note that the uncertainties of the loss tangents of Ligeia Mare (Mastrogiuseppe et al., 2018), Punga Mare, and the Kraken Mare's Baffin Sinus significantly overlap.

Considering the estimated composition of Punga Mare and using the Lorentz Lorenz formula (Born and Wolf, 1999), we derived the real part of the dielectric component of the mixture as $1.67^{+0.05}_{-0.05}$. This value is consistent with the low emissivity measured by the radiometry (Le Gall et al., 2016; Janssen et al., 2016) and is used as input to generate the bathymetry of the mare and constrain the seafloor roughness.

Results of the Monte Carlo estimates and relative uncertainties are reported in Fig. 3, which shows that the maximum depth for Punga Mare measured along the track is about 110 m. The derived along-track bathymetry is consistent with the observational evidence obtained from SAR images of both Punga Mare and Baffin Sinus (Figs. 1 and 2). The seafloor of Punga Mare shows a 50 meter elevation rise due to the presence of the central island visible from SAR images (see Fig. 2, upper-left panel). Moreover, there is an overall agreement between the derived seafloor profile and the bathymetry that would be qualitatively inferred from the morphology (e.g. shape of coastal features, presence of bays, distance from shorelines) of the mare and the brightness of the SAR images, if interpreted as a proxy for the seafloor depth. Based on the

Please cite this article in press as: Mastrogiuseppe, M., et al. Cassini radar observation of Punga Mare and environs: Bathymetry and composition. Earth Planet. Sci. Lett. (2018), https://doi.org/10.1016/j.epsl.2018.05.033

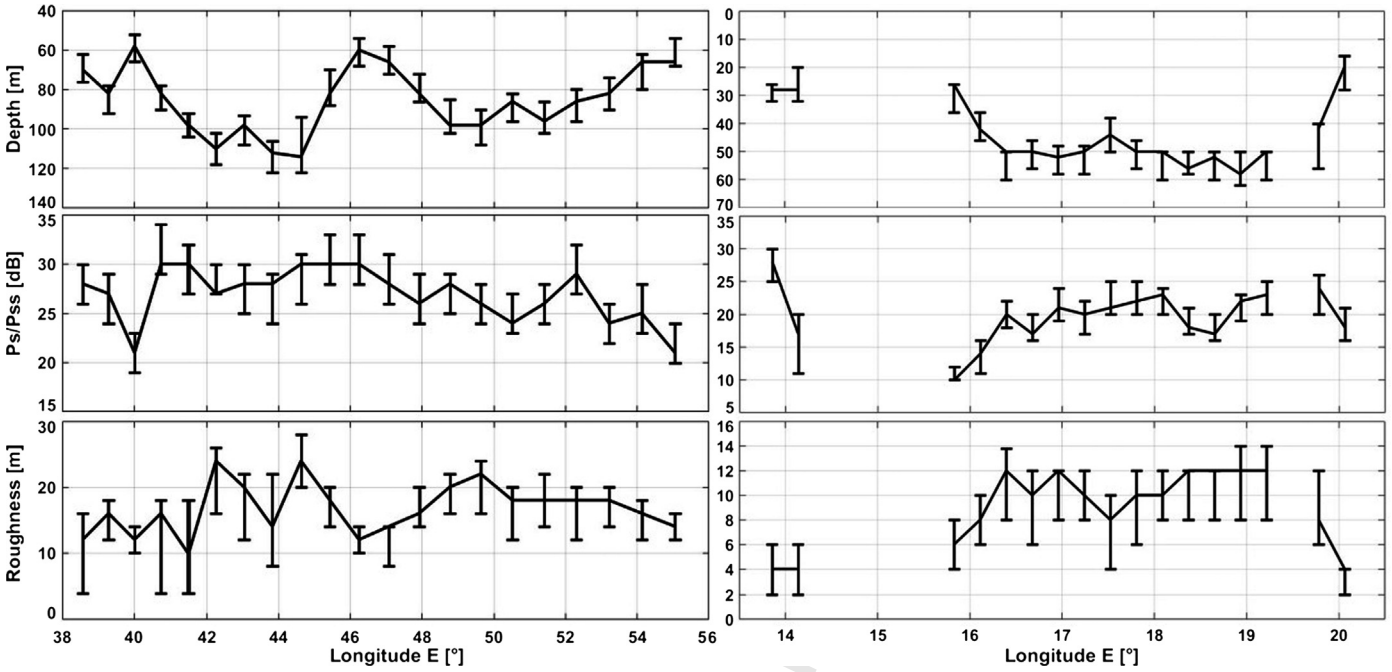

Fig. 3. Estimated depths (upper panels), surface-subsurface relative power (P_s/P_{ss}) (middle panels), and subsurface roughness (lower panels) for Punga Mare (left) and Baffin Sinus (right). Error bars are relative to 1-sigma uncertainty.

same qualitative considerations, the shallower bathymetry of North Kraken Mare at Baffin Sinus is also consistent with the morphology and brightness of this liquid body as observed from SAR images.

The depth of 110 m was measured at about 20–30 km from the nearest shoreline. This suggests a seabed profile that is rather steep, similar to that of the southern margin of Ligeia Mare as measured on T91 (Mastrogiuseppe et al., 2014a, 2014b), and rather steeper than the northern part of that transect (160 m over ~150 km). We note similarly that our bathymetric transect is at the southern margin of Punga Mare.

4. Seafloor backscattering: comparison of Punga and Ligeia Mare

In addition to the liquid composition, we use radar data for investigating dielectric properties of the seafloor. We compare seafloor backscattering of Punga Mare, observed during the T108, along with the backscattering of Ligeia Mare, measured using T91 flyby data. This comparison is particularly reliable since geometry and radar system parameters during the acquisition of the two observations were similar. We noted a remarkable similarity among echoes backscattered at the seafloor of the two seas, as shown with an example in Fig. 4. Radar waveforms indicate relative smooth topography (i.e. subsurface pulse shape approaches to a Gaussian single peak) and high transparency of the liquid (i.e. intensity ratio of surface and seafloor echoes is lower than 30 dB).

Considering the estimated specific attenuation K values of 13 dB/μs and 16 dB/μs for the Punga and Ligeia mare, respectively, we use formula (1) for a quantitative investigation of the sea floor composition of the two liquid bodies.

Formula (1) is used to relate the P_s/P_{ss} measurements with seafloor reflectivity R_{12}, surface reflectivity Γ_s, and attenuation K, assuming three possible values for the scattering term f_{ss}, which accounts for subsurface roughness scattering effects and can be expressed by rms slope. Such assumptions are necessary since the inversion problem is ill posed. For our study we derive the scattering terms f_{ss} using the Geometrical Optics (GO) formulation (Ulaby et al., 1982) along with three possible values of rms slopes ranging from 1° to 5°. Note that the rms slope values adopted here

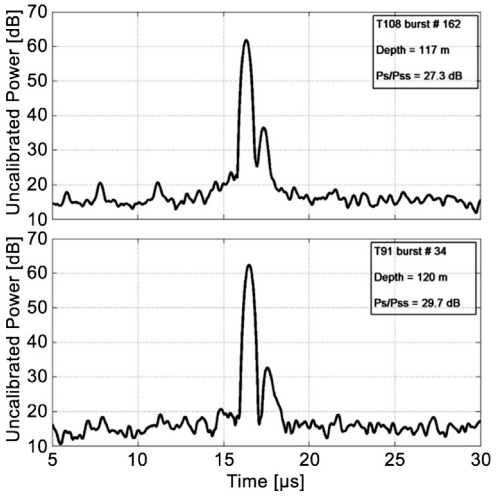

Fig. 4. Waveforms acquired during fly-by T108 over Punga (upper panel) and during fly-by T91 over Ligeia Mare (lower panel). Echoes backscattered from the seafloor are indicative of relative smooth topography at the resolution scale of the radar (35 m) and high transparency of the liquid.

are arbitrary and although they could represent the real values on Titan, they are only used in this study as reference values for comparing the dielectric properties of the two seafloors.

$$\left.\frac{P_s}{P_{ss}}\right|_{dB} = \Gamma_s|_{dB} - (1-\Gamma_s)^2|_{dB} - R_{12}|_{dB} + K|_{dB} + \left.\frac{f_s}{f_{ss}}\right|_{dB} \quad (1)$$

For each of the waveforms acquired over the two maria, inverting formula (1), we calculated a value of effective permittivity of the seafloor for different values of rms slope. The result is shown in Fig. 5 where the permittivity of the two seafloors is plotted along the radar transect of T91 and T108. We note that Ligeia Mare and Punga Mare seafloors show similar values of effective permittivity for similar values of small scale roughness. Moreover, the shape of radar waveforms suggests they have similar seafloor topography. Our conclusion is that the seafloors of both these maria are relatively smooth at the resolution scale of the radar (35 m)

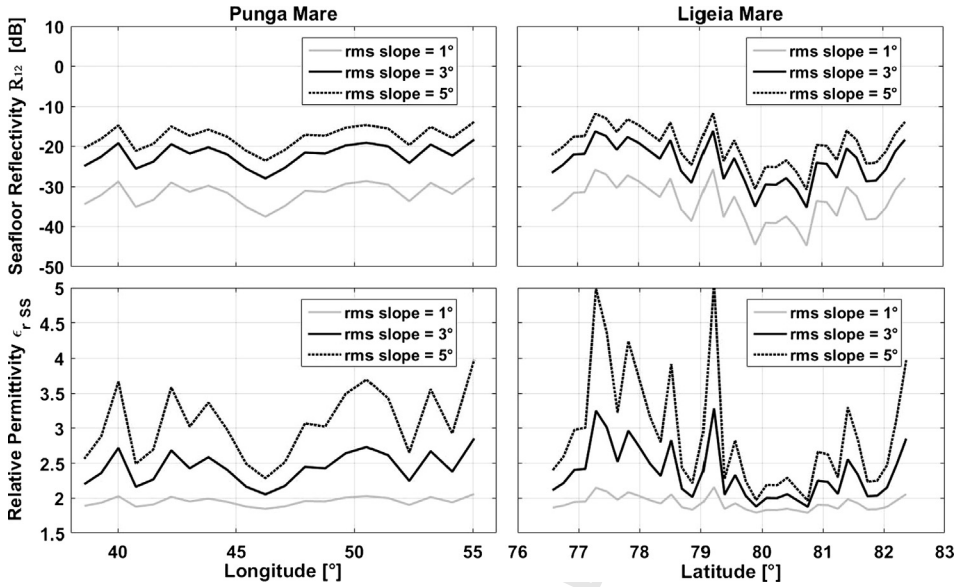

Fig. 5. Comparison between the seafloor reflectivity and the relative dielectric constant for Punga and Ligeia Mare for three possible values of rms slope. (Left column) Punga Mare. (Right column) Ligeia Mare.

and considering the adopted values for the microscale roughness, the composition of the two sea floors is consistent with several possible materials present on Titan, such as solid organics, water ice or a mixture of these materials. The roughness of the sea floors is smoother than that of terrain immediately surrounding the maria, consistent with sediment deposition throughout the observed sea floor.

5. Summary and implications

We analyzed the flyby T108 radar altimetry data acquired over Punga Mare and Baffin Sinus. The detection of the seafloor allowed us to investigate the liquid composition, the bathymetry, and seafloor topography of these liquid bodies. We found that the loss tangents of Punga Mare and Baffin Sinus are similar to that of Ligeia Mare within the 1-sigma uncertainty of the estimates ($\tan\delta = 4.4^{+0.9}_{-0.9} \times 10^{-5}$ for Ligeia Mare, $3^{+1}_{-1} \times 10^{-5}$ for Punga Mare and $3^{+1}_{-2} \times 10^{-5}$ for Baffin Sinus. See Supplementary Table 1 for relative composition values. However, the best fit values obtained here suggest that the composition for Punga Mare and Baffin Sinus might be most consistent with a binary methane-nitrogen system, with nitrogen approaching its solubility limit of 20% mole fraction in liquid methane and with little or no ethane or higher order hydrocarbons.

Several scenarios have been proposed which could permit ethane-poor seas. Mousis et al. (2016) and Choukroun et al. (2010) suggested that ethane might be sequestered by clathration if the crust of water ice or methane hydrates is exposed at the sea bed, resulting in methane-dominated liquids. However, this effect does not have any a priori latitude dependence.

The hydrological scenario proposed by Lorenz (2014) predicts an equator-to-pole gradation in methane and nitrogen abundance in the seas, much as salinity varies, e.g., between the Black Sea and the Mediterranean (or the Baltic and North Sea) on Earth. Higher inputs of 'fresh' liquid (on Titan, methane), either by higher rainfall rates and/or by larger land catchment areas, can displace solutes (salt, or ethane) to other basins in a system of connected seas. Although the simple model in Lorenz (2014) did not consider Punga specifically (at the time its hydraulic connection to the other seas was not obvious), the paradigm in that paper qualitatively suggests that the near-polar Punga Mare should be most ethane-poor, since circulation models suggest methane precipitation on Titan increases with latitude, and as the smallest sea, Punga Mare may have a proportionately larger catchment area, both factors favoring efficient flushing of solutes (the ethane and propane etc. which would predict higher loss tangents) into Kraken.

Alternatively, the latitudinal difference in composition could be explained as the results of the gradient in the surface temperature, assuming thermodynamic equilibrium with an atmosphere with constant methane mixing ratio (Tan et al., 2015; Tan and Kargel, 2018).

Particularly, using models of cryogenic chemical systems, Tan et al. (2015) suggested that latitudinal (e.g. two Kelvin difference in temperature from pole to 20 degrees of latitude) and seasonal variation of surface temperature could determine variations in vapor density and equilibrium phase compositions on Titan, thus affecting the atmospheric dynamics as well as the global fluid circulation in the surface and upper crust. More specifically, the authors predict more abundant but less dense liquid in large seas at higher latitude. These methane-rich liquids will tend to flow toward lower, warmer latitudes, re-equilibrating on the way to the equator with the lower atmosphere through evaporation of methane and thus a progressive enrichment of ethane at the lower latitude. Finally, ethane-richer, denser liquid would sink to the bottom of the sea and then flow poleward in a density-controlled cycle analogous to thermohaline circulation systems on Earth (Tan et al., 2015). However this thermally-driven local-thermodynamic equilibrium circulation scenario, fails to predict the compositions we have observed, but rather is too ethane-rich in the northern seas. These models also predict the presence of higher order components, such as propane, which would further increase absorptivity and likely make the models incompatible with observed loss tangents. Based on these observations, it appears that non-equilibrium processes are key to understanding Titan, as on Earth, where the atmospheric humidity is not 100% despite being a largely water-covered planet.

Given that the loss tangents obtained so far are the same in a formal (one sigma) sense, it may in fact be challenging to properly infer any compositional variability of seas until the composition and depth of Kraken Mare, by far the largest liquid reservoir, are determined.

To better constrain the uncertainties regarding this variability, new orbital missions equipped with multi-frequency radar dedi-

cated to map composition of Titan seas and lakes are envisaged. Additionally, direct measurements of composition and dielectric properties by one or more in-situ probes (Lorenz and Mann, 2015) could provide ground truth to robustly infer composition globally from radar data. Therefore, a combination of orbital data along with in situ direct measurements would represent the most efficient exploration effort.

While this effort requires future missions (orbital or landed) to Titan, it is remarkable that the Cassini mission (and its radar in particular), although not conceived for such measurements, has been able to obtain depths and bulk liquid compositions of lakes and seas with only a handful of observations.

Acknowledgements

M.M. and R.S. would like to acknowledge support from Italian Space Agency (ASI) grant 2014-041-R.0; G.D.A. was supported by the Italian Ministry of University and Research through FIRB-RBFR130ICQ grant. M.M., A.G.H., and V.P. would like to acknowledge support from NASA CDAP grant NNX15AH10G; R.L. acknowledges NASA grants NNX13AH14G and NNX13AK97G. J.I.L. is grateful for the ministrations of the Cassini mission in supporting his research. We appreciate the efforts of the Cassini TOST (Titan Orbiter Science Team) and RADAR Team in planning and executing these observations, in particular Yanhua Anderson and Richard West took great care to implement the spacecraft turns and instrument settings to achieve the Punga inspection reported here.

Appendix A. Supplementary material

Supplementary material related to this article can be found online at https://doi.org/10.1016/j.epsl.2018.05.033.

References

Alberti, G., Festa, L., Papa, C., Vingione, G., 2009. A waveform model for near-Nadir radar altimetry applied to the Cassini mission to Titan. IEEE Trans. Geosci. Remote Sens. 47 (7), 2252–2261. https://doi.org/10.1109/TGRS.2009.2012718.

Barnes, J.W., Sotin, C., Soderblom, J.M., et al., 2014. Planet. Sci. 3 (3). https://doi.org/10.1186/s13535-014-0003-4.

Blackman, R.B., Tukey, J.W., 1959. Particular pairs of windows. In: The Measurement of Power Spectra, from the Point of View of Communications Engineering. Dover, New York, pp. 98–99.

Birch, S.P.D., Hayes, A.G., Dietrich, W.E., Howard, A.D., Bristow, C.S., Malaska, M.J., Lopes, R.M.C., 2017. Geomorphologic mapping of Titan's polar terrains: constraining surface processes and landscape evolution. Icarus 282, 214–236. https://doi.org/10.1016/j.icarus.2016.08.003.

Born, M., Wolf, E., 1999. Principles of Optics: Electromagnetic Theory of Propagation, Interference and Diffraction of Light, 7th ed. Cambridge University Press. ISBN 0-521-64222-1, section 2.3.3.

Buono, K.M., 1992. A Bandwidth Extrapolation Technique for Improved Range Resolution of Coherent Radar Data. Project Report CJP-60, Revision 1, MIT Lincoln Laboratory.

Choukroun, M., Grasset, O., Tobie, G., Sotin, C., 2010. Stability of methane clathrate hydrates under pressure: influence on outgassing processes of methane on Titan. Icarus 205 (2), 581–593. https://doi.org/10.1016/j.icarus.2009.08.011.

Elachi, C., et al., 2004. Radar: the Cassini Titan radar mapper. Space Sci. Rev. 115 (1), 71–110. Available http://link.springer.com/article/10.1007%2Fs11214-004-1438-9 [Online].

Grima, C., Mastrogiuseppe, M., Hayes, A.G., Wall, D.S., Lorenz, R.D., Hofgartner, J.D., Stiles, B., Elachi, C., 2017. Surface roughness of Titan's hydrocarbon seas. Earth Planet. Sci. Lett. (ISSN 0012-821X) 474, 20–24. https://doi.org/10.1016/j.epsl.2017.06.007.

Hayes, A.G., 2016. The lakes and seas of Titan. Ann. Rev. Earth Space Sci. 44 (1), 57–83.

Hayes, A.G., Aharonson, O., Callahan, P., Elachi, C., Gim, Y., Kirk, R., Lewis, K., Lopes, R., Lorenz, R., Lunine, J., Mitchell, K., Mitri, G., Stofan, E., Wall, S., 2008. Hydrocarbon lakes on Titan: distribution and interaction with a porous regolith. Geophys. Res. Lett. 35, 9204.

Hayes, A.G., Lorenz, R.D., Donelan, M.A., Manga, M., Lunine, J.I., Schneider, T., Lamb, M.P., Mitchell, J.M., Fischer, W.W., Graves, S.D., Tolman, H.L., Aharonson, O., Encrenaz, P.J., Ventura, B., Casarano, D., Notarnicola, C., 2013. Wind driven capillary-gravity waves on Titan's lakes: hard to detect or non-existent? Icarus (ISSN 0019-1035) 225 (1), 403–412. https://doi.org/10.1016/j.icarus.2013.04.004.

Hayes, A.G., Birch, S.P.D., Dietrich, W.E., Howard, A.D., Kirk, R.L., Poggiali, V., Mastrogiuseppe, M., Michaelides, R.J., Corlies, P.M., Moore, J.M., Malaska, M.J., Mitchell, K.L., Lorenz, R.D., Wood, C.A., 2017. Topographic constraints on the evolution and connectivity of Titan's lacustrine basins. Geophys. Res. Lett.

Iess, L., et al., 2012. The tides of Titan. Science 337, 457. https://doi.org/10.1126/science.1219631.

Janssen, M.A., Le Gall, A., Lopes, R.M., Lorenz, R.D., Malaska, M.J., Hayes, A.G., Neish, C.D., Solomonidou, A., Mitchell, K.L., Radebaugh, J., Keihm, S.J., Choukroun, M., Leyrat, C., Encrenaz, P.J., Mastrogiuseppe, M., 2016. Titan's surface at 2.18-cm wavelength imaged by the Cassini RADAR radiometer: results and interpretations through the first ten years of observation. Icarus (ISSN 0019-1035) 270, 443–459. https://doi.org/10.1016/j.icarus.2015.09.027.

Le Gall, A., et al., 2016. Composition, seasonal change, and bathymetry of Ligeia Mare, Titan, derived from its microwave thermal emission. J. Geophys. Res., Planets 121, 233–251. https://doi.org/10.1002/2015JE004920.

Lopes, R.M.C., et al., 2013. Cryovolcanism on Titan: new results from Cassini RADAR and VIMS. J. Geophys. Res., Planets 118, 416–435. https://doi.org/10.1002/jgre.20062.

Lorenz, R.D., 2014. The flushing of Ligeia: composition variations across Titan's seas in a simple hydrological model. Geophys. Res. Lett. 41, 5764–5770. https://doi.org/10.1002/2014GL061133.

Lorenz, R.D., Mann, J., 2015. Seakeeping on Ligeia Mare: dynamic response of a floating capsule to waves on the hydrocarbon seas of Saturn's Moon Titan. Johns Hopkins APL Tech. Dig. 33 (2), 82–94.

Malaska, M.J., Hodyss, R., Lunine, J.I., Hayes, A.H., Hofgartner, J.D., Hollyday, G., Lorenz, R.D., 2017. Laboratory measurements of nitrogen dissolution in Titan lake fluids. Icarus (ISSN 0019-1035) 289, 94–105. https://doi.org/10.1016/j.icarus.2017.01.033.

Mastrogiuseppe, M., et al., 2014a. The bathymetry of a Titan sea. Geophys. Res. Lett. 41, 1432–1437. https://doi.org/10.1002/2013GL058618.

Mastrogiuseppe, M., et al., 2014b. Titan dune heights retrieval by using Cassini radar altimeter. Icarus (ISSN 0019-1035) 230, 191–197. https://doi.org/10.1016/j.icarus.2013.09.028.

Mastrogiuseppe, M., et al., 2016. Radar sounding using the Cassini altimeter: waveform modeling and Monte Carlo approach for data inversion of observations of Titan's seas. IEEE Trans. Geosci. Remote Sens. 54 (10). https://doi.org/10.1109/TGRS.2016.2563426.

Mastrogiuseppe, M., et al., 2018. Bathymetry and composition of Titan's Ontario Lacus derived from Monte Carlo-based waveform inversion of Cassini RADAR altimetry data. Icarus (ISSN 0019-1035) 300, 203–209. https://doi.org/10.1016/j.icarus.2017.09.009.

Mitchell, K.L., Barmatz, M.B., Jamieson, C.S., Lorenz, R.D., Lunine, J.I., 2015. Laboratory measurements of cryogenic liquid alkane microwave absorptivity and implications for the composition of Ligeia Mare, Titan. Geophys. Res. Lett. 42, 1340–1345. https://doi.org/10.1002/2014GL059475.

Mitri, G., Bland, M.T., Showman, A.P., Radebaugh, J., Stiles, B., Lopes, R.M.C., Lunine, J.I., Pappalardo, R.T., 2010. Mountains on Titan: modeling and observations. J. Geophys. Res. 115, E10002. https://doi.org/10.1029/2010JE003592.

Mousis, O., Lunine, J.I., Hayes, A.G., Hofgartner, J.D., 2016. The fate of ethane in Titan's hydrocarbon lakes and seas. Icarus.

Poggiali, V., et al., 2016. Liquid-filled canyons on Titan. Geophys. Res. Lett. 43, 7887–7894. https://doi.org/10.1002/2016GL069679.

Radebaugh, J., et al., 2007. Mountains on Titan observed by Cassini Radar. Icarus (ISSN 0019-1035) 192 (1), 77–91. https://doi.org/10.1016/j.icarus.2007.06.020.

Stofan, E.R., 2007. The lakes of Titan. Nature 445, 61–64. Available http://www.nature.com/nature/journal/v445/n7123/abs/nature05438.html [Online].

Tan, S.P., Jeffrey, S.K., Donald, E.J., Mastrogiuseppe, M., Hertanto, A., Marion, G.M., 2015. Titan's liquids: exotic behavior and its implications on global fluid circulation. Icarus (ISSN 0019-1035) 250, 64–75. https://doi.org/10.1016/j.icarus.2014.11.029.

Tan, S.P., Kargel, J.S., 2018. Multiphase-equilibria analysis: application in modeling the atmospheric and lacustrine chemical systems of Saturn's moon Titan. Fluid Phase Equilib. (ISSN 0378-3812) 458, 153–169. https://doi.org/10.1016/j.fluid.2017.11.020.

Ulaby, F.T., Moore, R.K., Fung, A.K., 1982. Microwave Remote Sensing, vol. 2. Addison–Wesley, Reading, MA (Chapters 11 and 12).

West, R.D., et al., 2009. Cassini RADAR sequence planning and instrument performance. IEEE Trans. Geosci. Remote Sens. 47 (6), 1777–1795. https://doi.org/10.1109/TGRS.2008.2007217.

Wood, C.A., et al., 2010. Impact craters on Titan. Icarus (ISSN 0019-1035) 206 (1), 334–344. https://doi.org/10.1016/j.icarus.2009.08.021.

XMLVIEW: extended

Appendix A. Supplementary material

The following is the Supplementary material related to this article.

begin ecomponent begin ecomponent begin ecomponent begin ecomponent begin ecomponent begin ecomponent begin ecomponent begin ecomponent begin ecomponent begin ecomponent begin ecomponent begin ecomponent begin ecomponent begin ecomponent begin ecomponent begin ecomponent begin ecomponent

Label: MMC

caption: T108 Cassini RADAR observation: Geometry and System parameters.

link: **APPLICATION : mmc1**

end ecomponent end ecomponent

Sponsor names

Do not correct this page. Please mark corrections to sponsor names and grant numbers in the main text.

Italian Space Agency, *country*=Italy, *grants*=2014-041-R.0

NASA, *country*=United States, *grants*=NNX15AH10G

NASA, *country*=United States, *grants*=NNX13AH14G, NNX13AK97G

Highlights

- First bathymetric measurements of Punga mare, Titan's third-largest sea.
- Maximum depth measured along the track is about 110 m.
- Composition is consistent with 80% of methane and 20% of nitrogen.
- Little to no ethane is present on the mare.
- The moderate roughness of the sea floor is consistent with sediment deposition.

Please cite this article in press as: Mastrogiuseppe, M., et al. Cassini radar observation of Punga Mare and environs: Bathymetry and composition. Earth Planet. Sci. Lett. (2018), https://doi.org/10.1016/j.epsl.2018.05.033